Finite Element-Based Fatigue and Damage Assessment of Group Stud Shear Connectors in UHPC-Steel Composite Beams

Md Saddam Hussain
Department of Civil Engineering, NIT Patna, India
mdh.phd19.ce@nitp.ac.in (corresponding author)

Shambhu Sharan Mishra
Department of Civil Engineering, NIT Patna, India
ssmishra@nitp.ac.in

Received: 23 May 2025 | Revised: 30 June 2025 and 16 July 2025 | Accepted: 20 July 2025

 DOI: https://doi.org/10.48084/etasr.12313

ABSTRACT

This study investigates the static and fatigue performance of stud shear connectors embedded in Ultra-High-Performance Concrete (UHPC) for composite structures. Three stud arrangements, Type-I, Type-II, and Type-III are evaluated using nonlinear Finite Element Analysis (FEA), focusing on the stress distribution, damage evolution, and fatigue life prediction. The von Mises stress distribution revealed critical stress concentrations at the stud roots and UHPC-steel interface, with Type-III arrangement demonstrating the most uniform stress spread and effective load transfer. Progressive damage modeling revealed that failure initiated at the stud roots and propagated as the applied load increased. The fatigue analysis demonstrated a substantial enhancement in the fatigue life with increased stud embedment length and optimized stud arrangements. Among the configurations studied, the Type-III arrangement exhibited the most favorable stress distribution, characterized by a more uniform load transfer and minimal stress concentration per stud. The specimens with this configuration achieved fatigue lives of up to 323,594 cycles without any visible damage, underscoring its superior fatigue resistance and structural reliability. The findings confirm that the strategic optimization of the stud geometry and the use of group stud arrangements can improve the stress distribution and significantly enhance the durability and performance of the steel–UHPC composite connections under cyclic loading.

Keywords-stud shear connectors; push-out FE analysis; fatigue analysis; damage modeling; UHPC

I. INTRODUCTION

Steel-concrete composite structures are used in modern construction due to their exceptional load-bearing capacity, structural efficiency, and cost-effectiveness. Combining the tensile strength and ductility of steel with the compressive strength and stiffness of concrete results in enhanced performance during service. The shear connector, which ensures effective load transfer between steel and concrete, is the critical component to analyze in such systems. The headed stud connectors are widely used in practice due to their rapid welding process, economic advantages, and robust mechanical performance [1]. The primary function of these stud connectors is to prevent slipping and separation between the steel girder and concrete slab during service. This behavior of stud connectors during service is influenced by various parameters, such as the stud geometry (diameter, height, and aspect ratio), material, positioning, and the characteristics of the surrounding concrete environment [2]. The traditional design methods typically place headed studs within Normal-Strength Concrete (NSC), necessitating high concrete thickness to prevent brittle failure mechanisms, such as pry-out and splitting of the concrete [3]. However, this approach often results in increased overall structural weight and inefficient utilization of the studs' shear capacity, thus demanding more innovative solutions.

UHPC offers outstanding compressive strength, typically exceeding 120 MPa, along with exceptional durability and mechanical performance compared to NCS. Its dense microstructure, which is achieved through optimized particle packing techniques and the incorporation of fine powders and fibers, substantially improves its resistance to cracking, shrinkage, and environmental degradation [4]. The introduction of UHPC has enabled the development of innovative lightweight structures that utilize short stud connectors. These short studs with UHPC, demonstrate distinct mechanical behavior compared to the traditional long studs in NSC, including enhanced shear capacity and resistance to brittle failure modes [5]. Building on the advancements in UHPC technology, researchers have developed Ultra-High-Performance Fiber-Reinforced Concrete (UHPFRC) by

incorporating steel or synthetic fibers, resulting in enhanced ductility, fracture toughness, and energy absorption capacity. These improved properties are especially advantageous for structures located in seismic zones and for applications involving high-impact loads, where superior post-cracking performance and effective energy dissipation are crucial [6, 7]. Nevertheless, research focusing on the behavior of stud shear connectors in UHPC-steel composite systems remains relatively scarce, particularly in terms of the localized stress behavior, damage evolution, and interaction at the UHPC–steel interface. Further investigation in these areas is critical for gaining a deeper understanding of failure mechanisms and for refining the design strategies to create safer, more efficient structural systems [8, 9]. Static push-out and fatigue tests are crucial for assessing the shear performance and long-term durability of stud shear connectors in steel-concrete composite structures, particularly in bridges and infrastructure projects. Authors in [8] examined the performance of short shear studs embedded in steel thin UHPC composite structures, focusing on factors, such as stud arrangement, diameter, and concrete cover thickness. Through a combination of laboratory testing and FEA, the study evaluated the load-bearing capacity and tracked damage progression in UHPC. Notably, the findings highlighted that Type II stud arrangements offered an effective compromise between maximizing the strength and limiting the damage within the UHPC matrix.

Authors in [10] employed FEA to predict the fatigue life of headed shear studs, providing insights into stress distribution and fatigue behavior under cyclic loading. This complements the aforementioned experimental work by offering a numerical approach to the fatigue assessment. Authors in [11] developed fatigue-life equations still referenced in design standards. Authors in [12] identified a linear relationship between the stiffness degradation and fatigue life. Authors in [13] explored fatigue-induced reductions in the stud strength, offering crucial insights into the long-term performance deterioration. Authors in [14] investigated the low-cycle fatigue behavior, revealing that grouped stud arrangements result in uneven stress distributions and reduced fatigue life. It was found that corrosion significantly reduces the fatigue life of studs, and that the S-N curves for corroded studs are different from those of the non-corroded studs. Many researchers examined grouped studs under biaxial loading, demonstrating that such conditions enhance the shear stiffness but reduce the bending deformation [15, 16]. Authors in [17] analyzed the mechanical behavior of headed studs in composite truss joints, focusing on the shear force distribution within the group.

Utilizing FEA techniques to predict the static and fatigue performance of stud shear connectors in UHPC-steel composite beams is an efficient approach for optimizing the time and effort. From a standardization perspective, revised design guidelines for grouped studs in composite structures are essential to enhance safety and durability. Static and fatigue analyses are conducted in this study using Abaqus and FE-SAFE, respectively. The HCF conditions are applied to capture the effects of repetitive service loads and wind-induced stresses, aiming to provide a realistic simulation of the long-term structural behavior.

The investigation considered three distinct stud arrangements along with variations in the stud length to evaluate their impact on the shear performance. The steel material properties for static analysis were adopted from [18], and the fatigue properties from [19]. Default material models from FE-SAFE were utilized for fatigue analysis. All loading procedures were designed to comply with the established engineering practices, following the specifications outlined in Eurocode-4 [20].

II. MATERIAL AND MODELING

The present study focuses on evaluating the effects of stud arrangement and stud length, by maintain UHPC cover thickness at 15 mm in addition to the stud length. All specimens are designed and fabricated following Eurocode-4 [20] guidelines, comprising H-shaped steel girders, UHPC slabs, and short shear connectors. The I-section steel girders are modeled using an elastic–plastic material model, featuring a cross-section of 250 × 250 mm², a total height of 450 mm, and a uniform flange and web thickness of 10 mm. The UHPC layer modeled using the Concrete Damage Plasticity (CDP) model, has dimensions of 450×400×75 mm and is left unreinforced to isolate the performance of the short stud connectors. The thickness of UHPC is increased as per stud size to keep a constant cover thickness. The short studs, which play a critical role in transferring the shear forces between the steel girder and the UHPC layer, are welded with girder to prevent slip, as depicted in Figure 1. A summary of all FEA models is presented in Table I, including stud arrangements, lengths, and cyclic loading parameters.

TABLE I. SUMMARY OF THE FEA MODELS

SN	Loading	Stud arrangement	Stud length	Cyclic loading		
				P_{max}/P_u	P_{min}/P_u	$\Delta P/P_u$
S-1	Monotonic	Type - I	60	-	-	-
S-2		Type - II	60	-	-	-
S-3		Type - III	60	-	-	-
F-1	Fatigue	Type - I	60	0.60	0.35	0.25
F-2		Type - II	60	0.60	0.35	0.25
F-3		Type - III	60	0.60	0.35	0.25
F-4		Type - I	65	0.60	0.35	0.25
F-5		Type - II	65	0.60	0.35	0.25
F-6		Type - III	65	0.60	0.35	0.25
F-7		Type - I	70	0.60	0.35	0.25
F-8		Type - II	70	0.60	0.35	0.25
F-9		Type - III	70	0.60	0.35	0.25

The CDP model incorporated key parameters, such as the dilation angle (ψ) = 17°, eccentricity (ξ) = 0.1, and viscosity parameter (μ) = 0.0001, which define the plastic flow and damage evolution of the material. The yield surface was characterized by a shape factor (k_c) of 2/3, representing a circular yield surface in the deviatoric plane typical for concrete-like materials. The stress-strain behavior and damage variables of UHPC under tension and compression are obtained from [18] and input into Abaqus software. For the steel girder, an elastic-plastic material model was employed, with a Young's modulus of 207.13 GPa, a yield stress of 253.29 MPa, and a tensile strength of 425.03 Mpa. For the stud, an elastic-plastic material model was employed with a Young's modulus of 206 GPa, a yield stress of 345 MPa, and a tensile strength of 415 MPa. To simulate the material failure, the ductile damage criterion was utilized, with the stress triaxiality versus the equivalent plastic strain relationship.

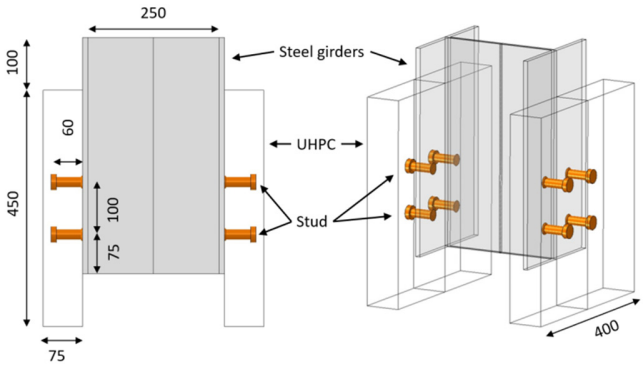

Fig. 1. Detailed CAD modeling of UHPC, girder, and studs for the slip test.

III. MESHING

A mesh convergence study was performed to determine the optimal mesh size while accurately capturing the FEA results of the stud shear connectors and the surrounding UHPC. Based on this analysis, a fine mesh with an element size of less than 2 mm is used around the stud roots, on the steel girder weld zone, and the adjacent concrete, as these regions are a major area of interest due to extreme deformations and the interaction between the UHPC and studs, as depicted in Figure 2. The remaining regions of UHPC are meshed with a coarser element size, a mesh size of approximately 5 mm. In Abaqus explicit C3D8R, the elements (8-node linear brick elements with reduced integration scheme) offer a good balance between computational efficiency and accuracy.

IV. LOAD AND BOUNDARY CONDITIONS

In static push-out tests, the applied load is gradually increased until failure to determine the ultimate shear capacity of the stud shear connectors with different arrangements and lengths. The failure typically occurs due to stud fracture, concrete crushing, or excessive slip between the steel and concrete interface. The maximum load recorded before failure is considered the static shear strength (Pu) of the stud. The loading process follows standard design codes, such as Eurocode-4 [20], to estimate the shear resistance of the studs.

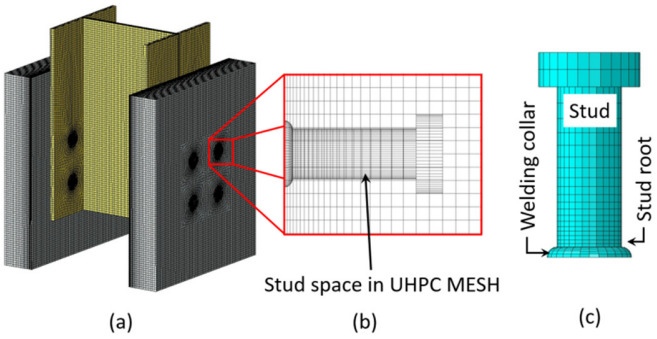

Fig. 2. (a) Meshed model of the assembly, (b) refined mesh of UHPC around the stud interface and girder, and (c) stud mesh.

Figure 3 (b) illustrates the cyclic loading procedure applied to the stud shear connectors in UHPC-steel composite beams, corresponding to the test parameters summarized in Table I. The fatigue tests are performed using cyclic loading at a frequency of 2.5 Hz [19], with an initial magnitude equivalent to one-third of P_u, as shown in Figure 3 (b). The peak load (P_{max}) is set at 60% of P_u (P_{max}/P_u =0.6). The minimum cyclic load (P_{min}) is 35% of P_u (P_{min}/P_u =0.35). The load range ΔP is set at 25% of Pu ($\Delta P/P_u$ =0.25). The loading rate in static tests is typically controlled within 0.02–0.05 mm/s slip displacement, as proposed by EN 1994-1-1 (Eurocode 4).

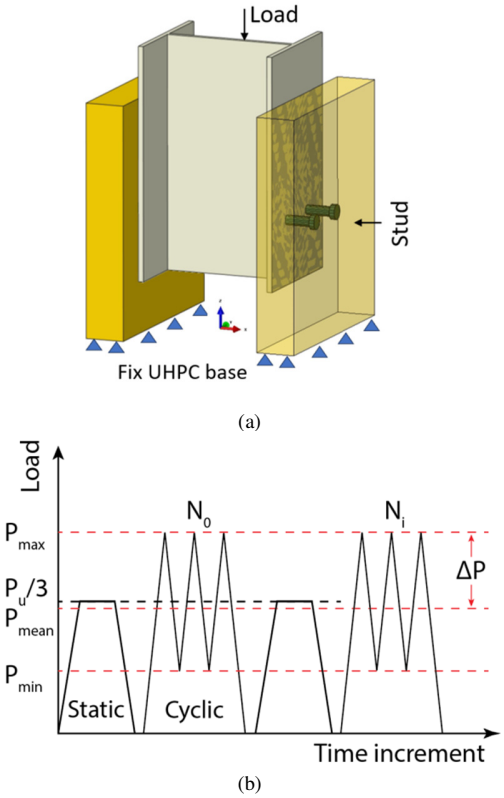

Fig. 3. (a) Slip test FE setup with displacement load and fix UHPC boundary conditions. (b) Cyclic loading protocol used in fatigue testing.

A full model with boundary conditions is illustrated in Figure 3 (a). The bottom surface of the UHPC block was fixed ($u_x = u_y = u_z = 0$) to prevent any movement. The displacement-controlled load is defined on the top surface of the steel girder. To model the contact behavior between the stud and UHPC, an interaction was defined. A friction coefficient of 0.4 was assigned for the interaction between the stud surface and UHPC, whereas the girder-UHPC interface was modeled with a friction coefficient of 0.73. The shear stress (τ) at the interface was governed by $\tau \leq \mu\sigma_n$, where σ_n is the normal contact pressure.

V. VALIDATION

To validate the results of the present study, the simulation results are validated against the findings of [21]. The comparison focused on a configuration featuring a 25 mm diameter stud, closely resembling the experimental setup. The FE model demonstrated a good agreement with the experimental findings, particularly with reaction forces and slip relation, as depicted in Figure 4 (a).

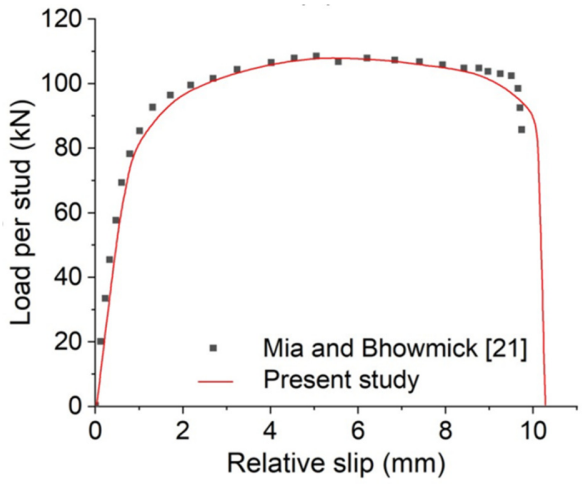

(a)

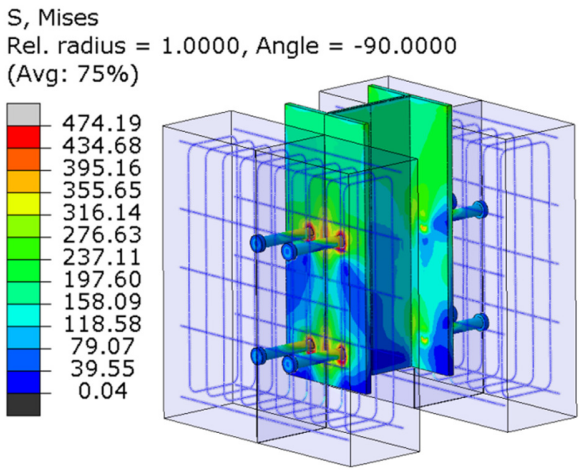

(b)

Fig. 4. (a) Comparison of load–slip behavior of the present study with the findings of [21]. (b) The von Mises stress distribution.

The von Mises stress distribution shown in the Figure 4 (b) highlights that the maximum stresses concentrate around the roots of the stud connectors, the critical locations where failure is most likely to initiate. This is due to the combined effects of the shear and bending stresses under the imposed displacement. The embedded reinforcement contributes to local confinement and helps distribute stress within the UHPC, but the studs remain the primary load-transferring elements. As loading progresses, stress accumulation at the stud roots increases, making them particularly prone to fatigue damage and potential fracture. After progressive progresses slip beyond the elastic limit, the strain hardening phase begins, where the force continues to rise at a reduced rate due to the strengthening of the material and increased interlocking between the stud and the UHPC. Following this peak, strain softening occurs, characterized by a sharp decline in force as the stud experiences plastic deformation, cracking in the UHPC, and potential partial failure at the stud root. This phase signifies the loss of stiffness and the transition toward failure. This trend was also verified in [22, 23].

VI. RESULTS AND DISCUSSION

A. Static Push-out Analysis Results

Figure 5 presents the von Mises stress distribution in the stud shear connectors and the surrounding UHPC and steel girder under shear loading conditions, ranging from 1.62 MPa to 417.50 Mpa. Stage (a) represents the unloaded condition. As the load gradually increased, notable stress develops at the root of the stud and along the UHPC-steel interface (stages b and c). Furthermore, by increasing the load, the stress levels at the stud root and the UHPC surrounding it reach their peak (stages d and e), close to the stud material's ultimate strength. The steel girder shows moderate stress levels, suggesting that the majority of the load is transferred to the UHPC. In the final stage (f), the stress distribution reveals damage in the stud, as indicated by the dotted lines. The root elements, with a stiffness degradation of 98% or more, are excluded from the FEA. The surroundings of UHPC also exhibit increased stress, indicating significant crushing in these areas. The steel girder maintains a lower stress profile, affirming that the failure is primarily governed by the behavior of the stud and UHPC interface.

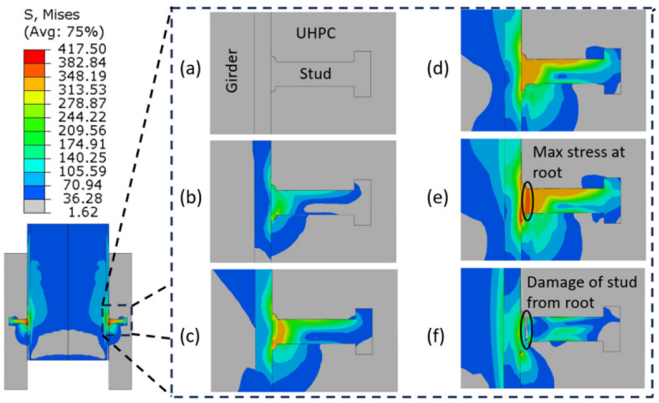

Fig. 5. The von Mises stress distribution in stud shear connectors.

The von Mises stress distribution is observed in three types of stud arrangement under shear loading. In Type-I stud arrangement, the stress is concentrated around the stud roots with minimal distribution into the UHPC, indicating a localized load transfer mechanism. Type-II arrangement, which includes additional studs, shows a relatively improved stress distribution, reducing the stress concentration around individual studs. However, Type-III arrangement demonstrates the most uniform stress distribution, with a stress spread over a larger UHPC volume. This indicates that the Type-III configuration enhances the load transfer efficiency and reduces the peak stress concentrations, potentially leading to improved structural performance and delayed failure initiation.

B. Progressive Damage in Stud Shear Connectors

Figure 6 illustrates the evolution of the damage in the stud connectors under shear loading, as predicted by the FEA. The color contours visually depict the progression of damage, ranging from 0.00 to 1.00. Notably, the damage is most severe around the stud roots and the UHPC-steel interface, where the stress concentrations are the highest.

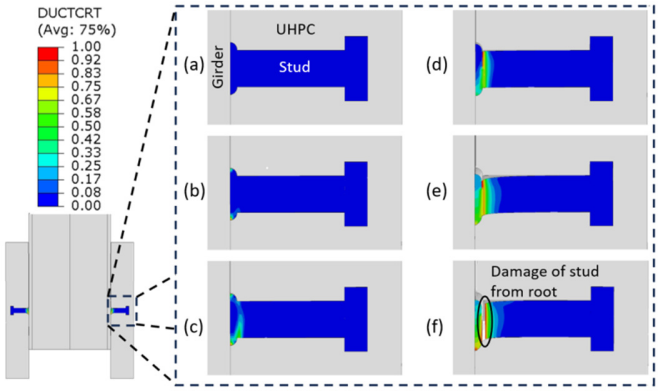

Fig. 6. Evolution of ductile damage in stud shear connectors.

In the initial stage (a), the stud displays no visible damage, suggesting that the materials are in an elastic state. As the load increases, the next stages (b and c) show damage initiation concentrated at the root of the stud, where the stress levels are highest, as seen Figure 5. In the subsequent stages (d and e), the damage propagates across the entire stud root, with severe damage concentrated at the corners of the stud. This signifies plastic deformation and localized failure in the surrounding UHPC. Finally, in the final stage (f), the damage becomes severe, and the stiffness of the element drops by 98%, rendering it incapable of sustaining further load. These elements deleted from the model demonstrate a complete damage at the stud root. It has been found that in push-out tests evaluating the UHPC-steel composite systems, failure typically arises from stud shank fracture coupled with localized UHPC crushing. For example, authors in [24] observed this failure mode in both static and fatigue tests of short-headed studs embedded in UHPC. Similarly, authors in [8] reported comparable findings in their investigation of short studs in steel-thin UHPC composite structures.

C. Prediction of Fatigue Life

The fatigue test results highlight the influence of the stud arrangement on the fatigue life of the UHPC-Steel Composite Beams. For specimen F-1, the stress range of 190.07 MPa resulted in a fatigue life of 12,882 cycles. Specimen F-2 with Type-II stud arrangement showed a fatigue life of 48,978 cycles at a stress range of 154.30 MPa. In contrast, the Type-III arrangement in specimen F-3 subjected to a lower stress range of 114.11 MPa demonstrated a significantly longer fatigue life of 239,883 cycles and showed no damage during the test. Similar trends are observed across the other specimens. For instance, specimen F-4, featuring a Type-I stud arrangement and subjected to a stress range of 183 MPa, endured 14,125 cycles. Specimen F-5, with a Type-II arrangement and a stress range of 139.27 MPa, sustained 57,544 cycles. Notably, specimen F-6, incorporating a Type-III stud arrangement, withstood 288,403 cycles under a stress range of 103.16 MPa without any signs of damage. These results indicate that Type-III stud arrangement offers a superior fatigue resistance compared to the Type-I and Type-II configurations, as it can endure significantly higher cycle counts.

TABLE II. FATIGUE ANALYSIS RESULTS

SN	Stud arrangement	Stress range (Mpa)	Min LOGLife -Repeats	Fatigue life, N_f (cycle)	Damage
F-1	Type-I	190.07	4.11	12882	7.76
F-2	Type-II	154.30	4.69	48978	2.04
F-3	Type-III	114.11	5.38	239883	0.42 (No damage)
F-4	Type-I	183.00	4.15	14125	7.08
F-5	Type-II	139.27	4.76	57544	1.74
F-6	Type-III	103.16	5.46	288403	0.35 (No damage)
F-7	Type-I	177.76	4.32	20893	4.49
F-8	Type-II	120.71	4.86	72444	1.38
F-9	Type-III	97.620	5.51	323594	0.31 (No damage)

The fatigue contour plots shown in Figure 7 illustrate the predicted fatigue life (in logarithmic scale, LOGLife-Repeats) of various stud configurations under different stud lengths and arrangements, as supported by the data summarized in Table II. Specimens F-1, F-4, and F-7 utilized Type-I stud arrangement with increasing stud lengths of 60 mm, 65 mm, and 70 mm, respectively. Despite these dimensional changes, Type-I consistently exhibited a high stress concentration and early fatigue failure, as evidenced by the low LOGLife values (ranging between 4.11 and 4.32) and relatively low cycle counts before failure (12,882-20,893 cycles). The damage values for these configurations are the highest, ranging from 4.49 to 7.76, indicating a significant material fatigue and vulnerability with respect to the stud length. However, in all FE experiments the cover thickness of UHPC maintained a constant value of 15 mm. Type-II configurations F-2, F-5, and F-8 demonstrated improved fatigue resistance, as presented in Figure 8. These arrangements showed increased fatigue lives (48,978-72,444 cycles), with corresponding higher LOGLife values (4.69-4.86) and lower damage indices (1.38-2.04). The stress concentration in Type-II studs was more distributed, resulting in a less severe fatigue accumulation compared to Type-I.

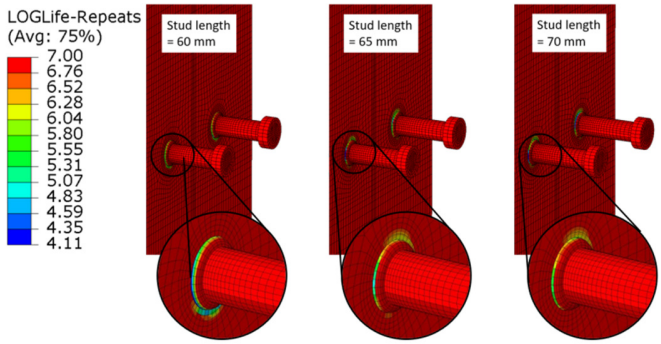

Fig. 7. Fatigue life contours for Type-I stud arrangement with lengths of 60 mm, 65 mm, and 70 mm.

The most favorable results are observed for specimens F-3, F-6, and F-9, which employed the Type-III stud arrangement. These configurations exhibited the highest fatigue lives—239,883-323,594 cycles—with LOGLife values between 5.38 and 5.51. Moreover, the damage indices are significantly lower (0.31-0.42), and no visible damage was detected during the simulation, as highlighted in the zoomed-in contours of F-3, F-6, and F-9. The fatigue stress distribution was more uniform around the weld collar and stud shank, thereby avoiding critical failure initiation points.

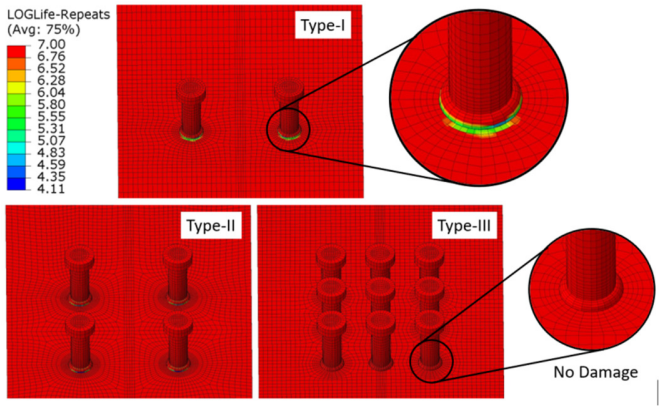

Fig. 8. Fatigue life contours for studs with Type-I, Type-II, and Type-III arrangements.

The cyclic stress (S_m) distribution results obtained from the FE-Safe simulations, as depicted in Figure 9, highlight the influence of the stud length and stud arrangement on the fatigue behavior. An increasing trend in the stud length from 60 mm to 70 mm demonstrates a clear reduction in the peak stress concentrations around the stud base and UHPC interface. Despite maintaining a constant UHPC cover thickness, the longer studs offer greater embedment depth within the UHPC, enhancing the mechanical interlock and increasing the bond area. This leads to more effective load transfer and a more uniform stress diffusion through the concrete, ultimately reducing the localized shear stress and the risk of fatigue crack initiation.

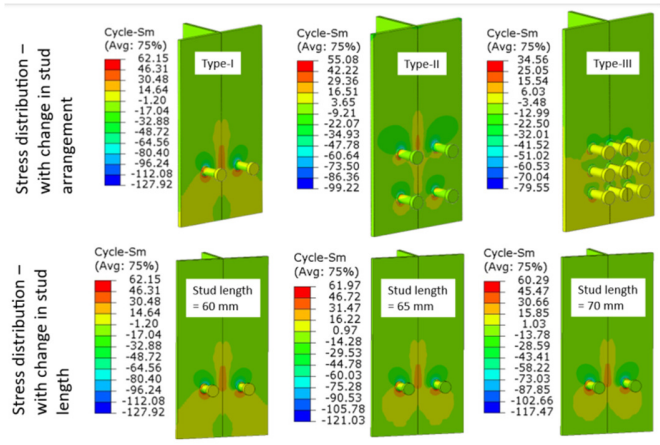

Fig. 9. Stress distribution contours (Cycle-S_m) for different stud arrangements (Type-I, Type-II, and Type-III) and varying lengths (60 mm, 65 mm, and 70 mm).

Type-I setup exhibits sharp and concentrated stress zones around each stud, indicating higher cyclic loads per stud and an increased potential for early fatigue failure. Type-II configuration shows a modest improvement, with stress being more evenly spread across the four studs, though notable concentrations still exist. In contrast, Type-III arrangement significantly improves the stress distribution, where the applied load is shared among nine studs. This uniform distribution minimizes the stress concentration per stud, thereby reducing the likelihood of fatigue damage. The absence of critical stress hotspots in the Type-III case explains the superior fatigue life observed in FEA.

VII. CONCLUSIONS

A comprehensive Finite Element Analysis (FEA) was carried out to investigate the behavior of stud shear connectors embedded in Ultra-High-Performance Concrete (UHPC) under static and cyclic shear loading. The study evaluated the stress distribution, failure mechanisms, fatigue life, and the effects of the stud length and arrangement. The key conclusions of this study are:

- Failure is primarily governed by high stress concentrations at the stud root and UHPC–steel interface, leading to stud shank fracture and localized UHPC crushing.
- The fatigue performance is significantly influenced by the stud configuration, with Type-I showing poor load distribution and early fatigue failure, Type-II offering modest improvement, and Type-III demonstrating superior load-sharing, reduced stress peaks, and significantly enhanced fatigue life.
- The fatigue life improved from 12,882 cycles (Type-I) to 323,594 cycles (Type-III) with minimal damage.
- Increasing the stud length from 60 mm to 70 mm enhanced the embedment, stress dispersion, and fatigue resistance.
- Type-III configuration with increased embedment depth is proposed for optimal fatigue performance and structural reliability in UHPC–steel composite systems.

This study is limited to a numerical investigation of the fatigue behavior under monotonic and cyclic loading. Furthermore, it can be extended to incorporate environmental factors, such as corrosion and temperature variation, strain rate sensitivity, and long-term degradation mechanisms, to simulate the real-world performance of UHPC–steel composite.

REFERENCES

[1] Z. Fang, S. Fang, and F. Liu, "Experimental and Numerical Study on the Shear Performance of Short Stud Shear Connectors in Steel–UHPC Composite Beams," *Buildings*, vol. 12, no. 4, Mar. 2022, Art. no. 418, https://doi.org/10.3390/buildings12040418.

[2] S. Wang, Z. Fang, Y. Ma, H. Jiang, and G. Zhao, "Parametric investigations on shear behavior of perforated transverse angle connectors in steel–concrete composite bridges," *Structures*, vol. 38, pp. 416–434, Apr. 2022, https://doi.org/10.1016/j.istruc.2022.01.015.

[3] J. Wang, Q. Xu, Y. Yao, J. Qi, and H. Xiu, "Static behavior of grouped large headed stud-UHPC shear connectors in composite structures," *Composite Structures*, vol. 206, pp. 202–214, Dec. 2018, https://doi.org/10.1016/j.compstruct.2018.08.038.

[4] J. Cao and X. Shao, "Finite element analysis of headed studs embedded in thin UHPC," *Journal of Constructional Steel Research*, vol. 161, pp. 355–368, Oct. 2019, https://doi.org/10.1016/j.jcsr.2019.03.016.

[5] J.-S. Kim, J. Kwark, C. Joh, S.-W. Yoo, and K.-C. Lee, "Headed stud shear connector for thin ultrahigh-performance concrete bridge deck," *Journal of Constructional Steel Research*, vol. 108, pp. 23–30, May 2015, https://doi.org/10.1016/j.jcsr.2015.02.001.

[6] Y. Shao, C.-W. Kuo, and C.-C. Hung, "Seismic performance of full-scale UHPC-jacket-strengthened RC columns under high axial loads," *Engineering Structures*, vol. 243, Sep. 2021, Art. no. 112657, https://doi.org/10.1016/j.engstruct.2021.112657.

[7] E. P. Sidodikromo, Z. Chen, and M. Habib, "Review of The Cement-Based Composite Ultra-High-Performance Concrete (UHPC)," *The Open Civil Engineering Journal*, vol. 13, no. 1, pp. 147–162, Nov. 2019, https://doi.org/10.2174/1874149501913010147.

[8] Y. Li *et al.*, "Shear behavior of short studs in steel-thin ultrahigh-performance concrete composite structures," *Case Studies in Construction Materials*, vol. 19, Dec. 2023, Art. no. e02423, https://doi.org/10.1016/j.cscm.2023.e02423.

[9] M. Shafieifar, M. Farzad, and A. Azizinamini, "Experimental and numerical study on mechanical properties of Ultra High Performance Concrete (UHPC)," *Construction and Building Materials*, vol. 156, pp. 402–411, Dec. 2017, https://doi.org/10.1016/j.conbuildmat.2017.08.170.

[10] A. Nakajima, I. Saiki, M. Kokai, K. Doi, Y. Takabayashi, and H. Ooe, "Cyclic shear force–slip behavior of studs under alternating and pulsating load condition," *Engineering Structures*, vol. 25, no. 5, pp. 537–545, Apr. 2003, https://doi.org/10.1016/S0141-0296(02)00165-7.

[11] R. Slutter and J. Fisher, "Fatigue strength of shear connectors," *Highway Research Record*, vol. 147, pp. 66–21, Jan. 1966.

[12] D. J. Oehlers and C. G. Coughlan, "The shear stiffness of stud shear connections in composite beams," *Journal of Constructional Steel Research*, vol. 6, no. 4, pp. 273–284, Jan. 1986, https://doi.org/10.1016/0143-974X(86)90008-8.

[13] G. Hanswille, M. Porsch, and C. Ustundag, "Resistance of headed studs subjected to fatigue loading," *Journal of Constructional Steel Research*, vol. 63, no. 4, pp. 475–484, Apr. 2007, https://doi.org/10.1016/j.jcsr.2006.06.035.

[14] C. Xu and K. Sugiura, "FEM analysis on failure development of group studs shear connector under effects of concrete strength and stud dimension," *Engineering Failure Analysis*, vol. 35, pp. 343–354, Dec. 2013, https://doi.org/10.1016/j.engfailanal.2013.02.023.

[15] C. Xu and K. Sugiura, "Analytical investigation on failure development of group studs shear connector in push-out specimen under biaxial load action," *Engineering Failure Analysis*, vol. 37, pp. 75–85, Feb. 2014, https://doi.org/10.1016/j.engfailanal.2013.11.010.

[16] C. Xu, K. Sugiura, H. Masuya, K. Hashimoto, and S. Fukada, "Experimental Study on the Biaxial Loading Effect on Group Stud Shear Connectors of Steel-Concrete Composite Bridges," *Journal of Bridge Engineering*, vol. 20, no. 10, Oct. 2015, Art. no. 04014110, https://doi.org/10.1061/(ASCE)BE.1943-5592.0000718.

[17] D. Y. Xue, Y. Q. Liu, S. F. Huang, and B. Ma, "Mechanical Behavior Study on Headed Studs for Composite Truss Joint," *Advanced Materials Research*, vol. 255–260, pp. 379–382, May 2011, https://doi.org/10.4028/www.scientific.net/AMR.255-260.379.

[18] J. Ding, J. Zhu, and T. Shi, "Performance of grouped stud connectors in precast steel-UHPC composite bridges under combined shear and tension loads," *Engineering Structures*, vol. 277, Feb. 2023, Art. no. 115470, https://doi.org/10.1016/j.engstruct.2022.115470.

[19] P. G. Lee, C. S. Shim, and S. P. Chang, "Static and fatigue behavior of large stud shear connectors for steel–concrete composite bridges," *Journal of Constructional Steel Research*, vol. 61, no. 9, pp. 1270–1285, Sep. 2005, https://doi.org/10.1016/j.jcsr.2005.01.007.

[20] Eurocode 4. Design of composite steel and concrete structures. General rules and rules for buildings, British Standards Institution, London, United Kingdom, Dec. 2004.

[21] Md. M. Mia and A. K. Bhowmick, "A finite element based approach for fatigue life prediction of headed shear studs," *Structures*, vol. 19, pp. 161–172, Jun. 2019, https://doi.org/10.1016/j.istruc.2019.01.001.

[22] H. Y. Loh, B. Uy, and M. A. Bradford, "The effects of partial shear connection in the hogging moment regions of composite beams Part II—Analytical study," *Journal of Constructional Steel Research*, vol. 60, no. 6, pp. 921–962, Jun. 2004, https://doi.org/10.1016/j.jcsr.2003.10.008.

[23] N. Gattesco and E. Giuriani, "Experimental study on stud shear connectors subjected to cyclic loading," *Journal of Constructional Steel Research*, vol. 38, no. 1, pp. 1–21, May 1996, https://doi.org/10.1016/0143-974X(96)00007-7.

[24] J. Cao, X. Shao, L. Deng, and Y. Gan, "Static and Fatigue Behavior of Short-Headed Studs Embedded in a Thin Ultrahigh-Performance Concrete Layer," *Journal of Bridge Engineering*, vol. 22, no. 5, May 2017, Art. no. 04017005, https://doi.org/10.1061/(ASCE)BE.1943-5592.0001031.